International Journal of General Medicine

Dovepress
Taylor & Francis Group

Open Access Full Text Article

ORIGINAL RESEARCH

Synergistic Effects of Thymoquinone, 3-Hydrazinoquinoxaline-2-Thiol, and Amphotericin B Against Methicillin-Resistant *Staphylococcus aureus*: In vitro and in silico Evaluation

Karem Ibrahem [1,2], Abdelbagi Alfadil [1]

[1]Department of Clinical Microbiology and Immunology, Faculty of Medicine, King Abdulaziz University, Jeddah, Saudi Arabia; [2]Department of Clinical Microbiology Laboratory, King Abdulaziz University Hospital, Jeddah, 21589, Saudi Arabia

Correspondence: Karem Ibrahem, Department of Clinical Microbiology and Immunology, Faculty of Medicine, King Abdulaziz University, Jeddah, Saudi Arabia, Tel 00 966 56 252 5685, Email kaibrahem@kau.edu.sa

Introduction: Bacterial infections continue to pose a major global health challenge, intensified by the increasing prevalence of antimicrobial-resistant pathogens such as Methicillin-resistant *Staphylococcus aureus* (MRSA). The emergence of resistance mechanisms, particularly the *mecA* gene encoding PBP2a, significantly reduces the effectiveness of existing antibiotics, including advanced agents like linezolid and daptomycin. Although vancomycin remains a cornerstone therapy, its variable tissue penetration and growing resistance emphasize the urgent need for alternative treatments. This study explores the potential synergistic effects of 3-hydrazinoquinoxaline-2-thiol (3HTQ), thymoquinone (THQ), and amphotericin B against clinical MRSA isolates.

Methods: Antibacterial activity was evaluated using broth microdilution and checkerboard assays. Molecular docking and molecular dynamics (MD) simulations were performed to assess binding interactions and complex stability. Minimum inhibitory concentrations (MICs) were determined for each compound and their combinations.

Results: Amphotericin B alone exhibited limited antibacterial activity with baseline MIC values ranging from 16–64 μg/mL; however, when combined with THQ and 3HTQ, the MIC values were markedly reduced—up to 32-fold in some MRSA isolates. Checkerboard analysis confirmed synergism, with fractional inhibitory concentration index (FICI) values ≤0.5. Molecular docking suggested potential interactions with key MRSA proteins, particularly PBP2a, while MD simulations indicated relative stability of these complexes.

Conclusion: The proposed mechanisms are based solely on in silico analyses and computational modeling, rather than direct biological or molecular experiments. These findings, supported by in vitro data and computational analyses, suggest that combining 3HTQ, THQ, and amphotericin B could be explored as a potential approach for managing MRSA infections and overcoming emerging antimicrobial resistance.

Keywords: MRSA, thymoquinone, amphotericin B, 3-hydrazinoquinoxaline-2-thiol, MIC, FICI, molecular docking

Introduction

Globally, bacterial infections continue to be a major health issue and a leading cause of mortality.[1] Antibiotic resistance, which limits the efficacy of antimicrobial therapies, further complicates this challenge.[2,3] The spread of resistant pathogens contributes to persistent infections and increased prevalence of disease.[4,5]

Several mechanisms allow bacteria to survive antimicrobial exposure, leading to antibiotic resistance.[6] For example, methicillin-resistant *Staphylococcus aureus* (MRSA) obtains resistance through the *mecA* gene, which encodes an altered penicillin-binding protein (PBP2a) with decreased affinity for β-lactam antibiotics.[7,8] A number of auxiliary factors are

https://doi.org/10.2147/IJGM.S603479
Received: 14 February 2026
Accepted: 6 May 2026
Published: 25 May 2026

also believed to contribute to the full MRSA resistance phenotype.[9] In spite of the introduction of newer antibiotics such as linezolid and daptomycin, resistance has already been reported.[10,11] Moreover, vancomycin remains a standard treatment for MRSA, but its tissue penetration is poor and resistant strains have emerged.[12]

Antibiotic resistance is further complicated by the slow pace of development of new antibiotics.[13] There has not been sufficient progress in the discovery of new antimicrobial agents to keep pace with the rapid appearance of resistance in bacteria.[14] Antibiotic research has been discouraged by high development costs, long development timelines, strict regulatory requirements, and low financial returns. As a result, the pipeline of new antibiotics remains limited, leaving few alternatives to replace increasingly ineffective ones.[9,10]

Given these challenges, there is a pressing demand for innovative therapeutic approaches and the development of novel antibiotics.[11] One promising approach is the use of combination therapies, where multiple antibiotics are administered together to enhance their effectiveness.[12] This strategy may help to overcome bacterial resistance mechanisms and achieve better treatment outcomes.

Drug discovery and target identification are increasingly guided by computational methods, especially in antimicrobial research, in addition to experimental approaches. A common application of molecular docking is to predict the binding mode of small molecules within protein active sites and to estimate the strength and stability of interactions between proteins and ligands. Using this method, it is possible to identify the most energetically favorable binding poses by efficiently and systematically exploring possible conformations. Before being validated experimentally, this technique allows an in-silico evaluation of protein-ligand interactions. Bioinformatics and computational biology have further improved docking accuracy, including predicting binding affinity and inhibitory constants.[15]

THQ is a naturally existing bioactive substance compound found in the seeds of Nigella sativa, commonly known as black cumin or black seed.[16] This compound is well-regarded for its anti-inflammatory, antioxidative, and anti-bacterial properties and anti-cancer.[17,18] THQ has shown significant anti-bacterial efficacy and notable anti-fungal activity against pathogens such as *Aspergillus niger* and *Candida albicans*.[18] Recently, number of simulation studies have provided compelling evidence suggesting that amphotericin B possesses significant inhibition potential against Methicillin-resistant *S. aureus* (MRSA). These studies have utilized a variety of computational techniques to model the interactions between amphotericin B and MRSA at a molecular level. Through detailed simulations, researchers have been able to observe how amphotericin B interacts with the bacterial cell membrane, potentially disrupting key processes essential for the bacteria's survival and proliferation. The findings from these simulations indicate that amphotericin B can effectively bind to specific targets within MRSA, thereby inhibiting its growth and reducing its pathogenicity. These results are promising and suggest that amphotericin B could be developed as a potential therapeutic drug against MRSA infections, addressing a significant challenge in the treatment of antibiotic-resistant bacterial infections.[19] Recently, 3HTQ has attracted attention as a potential antimicrobial agent. Previous studies have reported its activity against a range of microbial pathogens, including both bacterial and fungal species such as *Candida* spp, suggesting a broad antimicrobial spectrum. Moreover, evidence indicates that 3HTQ may enhance the efficacy of conventional antibiotics, including penicillin or vancomycin, when used in combination against MRSA, highlighting its potential role in combination-based therapeutic strategies.[16,20,21]

We hypothesized that quinoxaline derivatives, particularly 3-hydrazinoquinoxaline-2-thiol (3HTQ), might exhibit synergistic activity when combined with thymoquinone (THQ) and amphotericin B against clinical MRSA strains. Therefore, the aim of this study was to assess the in vitro antimicrobial activity and potential synergistic effects of these compounds against clinical isolates of MRSA through MIC determination, checkerboard assays, and complementary in silico analyses.

Materials and Methods

Bacterial Strains, Growth Media and Condition

This investigation consisted of comprehensive analysis of 18 MRSA species obtained from King Abdulaziz University Hospital in Jeddah, Saudi Arabia. These bacteria were meticulously maintained in glycerol and kept at a temperature of −80°C to maintain their viability over time. Prior to testing, a systematic thawing process was conducted, after which the

bacteria were cultivated on blood media plates sourced from HiMedia, India. The cultivation process was carried out overnight at a temperature of 37°C under aerobic conditions to ensure optimal growth and viability of the bacterial cultures. The sample collection and handling procedures strictly adhered to the guidelines set forth by the ethics and research committee of the Faculty of Applied Medical Sciences at King Abdulaziz University.

BACT/Alert VIRTUO and BioFire BCID2 panels were used in the initial detection process. Subcultures were carried out on 5% sheep blood agar, and species identification was performed using the VITEK 2 system. GeneXpert was used for detection of the mecA gene, as well as disk diffusion testing and mannitol salt agar supplemented with oxacillin for phenotypic confirmation of MRSA. The VITEK 2 AST-GP card (P580) was used for antimicrobial susceptibility testing (AST).

The study was conducted in accordance with the ethical approval number 38–712-456 and was fully compliant with the principles outlined in the Declaration of Helsinki, which governs the ethical standards for research involving human subjects. The ethical approval for accessing the de-identified clinical isolates data was granted on 09/08/2017. These procedures did not involve the collection of any patient identifiers such as names, ages, or nationalities. We did not have access to any patient information and only worked with bacterial cells. Consequently, the ethics committee decided that informed consent was not needed for the current study, as the use of these de-identified clinical isolates posed no risk to patient privacy or confidentiality. Overall, this careful and ethically sound approach ensured the integrity of the research process and the reliability of the findings derived from the analysis of the MRSA isolates.

Antibacterial Agents

This study focused on evaluating the efficacy of various antibacterial agents specifically against MRSA strains. Among the compounds tested, a novel 3HTQ compound was sourced from Fluorochem Ltd., a reputable supplier based in the United Kingdom. In addition to 3HTQ, we also examined the effects of thymoquinone and amphotericin B, both of which were obtained in powder form from Sigma-Aldrich, a globally recognized chemical supply company.

To ensure the accurate preparation and administration of these compounds, both 3HTQ and thymoquinone, as well as amphotericin B, were dissolved in 5% dimethyl sulfoxide (DMSO). This solvent was chosen due to its ability to effectively dissolve a wide range of organic compounds while maintaining the stability and activity of the antibacterial agents.

The selection and preparation of these agents were done with careful consideration to detail to ensure the reliability and reproducibility of the experimental results. By utilizing high-quality compounds and appropriate solvents, we aimed to generate robust data on the antibacterial efficacy of these agents against MRSA, thereby contributing valuable insights to the field of antimicrobial research. The stock solution of each antimicrobial agent was prepared at a concentration of 10 mg/mL. The initial working concentration before performing the double dilution method was 128 µg/mL for 3HTQ and 256 µg/mL for both Amphotericin B and THQ. The dilutions were prepared using the standard C1V1 = C2V2 equation to ensure accurate concentration adjustments.

Susceptibility Test via Broth Microdilution Assay

To analyse the antimicrobial sensitivity of the specific agents 3HTQ, THQ, and amphotericin B, we conducted a comprehensive broth microdilution test. This meticulous procedure involved generating a series of two-fold serial dilutions of the antimicrobial agents within Mueller Hinton Broth (MHB), which was procured from Sigma-Aldrich in the United States. These serial dilutions were carefully prepared to ensure accurate and consistent concentration gradients for each antimicrobial agent.

Following the preparation of the serial dilutions, 100 µL of each antimicrobial mixture was precisely filled into individual wells of 96-well microtiter plates. To achieve a standardized inoculum density, the mixture was diluted to match a 0.5 McFarland standard using a Biosan Densitometers DEN-1B suspension turbidity detector. This adjustment was crucial for maintaining uniformity across all test samples and ensuring reliable results. Following this a 5 µL of the prepared bacterial inoculum was transferred to the corresponding well supplemented with different concentrations of the antimicrobial agents. The inoculated plates were then incubated for 20 hours at 37°C to allow for bacterial growth and

interaction with the antimicrobial agents. This incubation period was essential for determining the effectiveness of the agents in inhibiting bacterial proliferation.

The antimicrobial susceptibility testing was rigorously done in triplicate to attain the accuracy and reproducibility of the findings. The mean values acquired from these triplicate tests were noted and analysed to determine the Minimum Inhibitory Concentrations (MICs) of the antimicrobial agents. The MIC is considered as the lowest concentration of a drug that is able of inhibiting the visible growth of a micro-organism. The MIC outcomes for the three anti-bacterial drugs were determined utilising the broth microdilution technique and interpreted according to the guidelines set by the Clinical and laboratory standard institutes (CLSI). These guidelines provide a standardized framework for conducting and interpreting antimicrobial susceptibility tests, ensuring that our results are both reliable and comparable to other studies in the field. By adhering to these rigorous procedures and standards, we aimed to generate robust and reliable data on the antimicrobial sensitivity of 3HTQ, thymoquinone, and amphotericin B against MRSA strains, thereby contributing valuable insights to the ongoing efforts in combating multidrug-resistant bacterial infections. Each test was done in three times and the average was estimated.[17,18]

Checkerboard Assay

To thoroughly assess the interactions among the antimicrobial agents 3HTQ, THQ, and amphotericin B, we employed the checkerboard broth assay. This method allows for the evaluation of potential synergistic effects between multiple antimicrobial compounds. The procedure began with the preparation of a twofold serial dilution of each antimicrobial compound in Mueller Hinton Broth (MHB), which was sourced from a reputable supplier. After preparing the serial dilutions, 33 µL of each dilution was carefully dispensed into the wells of 96-well microtiter plates. Ensuring precise inoculum-density, the bacterial mixture was diluted to a 0.5 McFarland standard using a Biosan Densitometer DEN-1B suspension turbidity detector. This step was crucial for maintaining consistency and accuracy across all experimental conditions. Following this adjustment, five µL of the diluted bacterial inoculum was transferred into each well having the various concentrations of the antimicrobial agents. Plates were incubated at 37°C for 20 hours.

To evaluate the synergy between 3HTQ, THQ, and amphotericin B, we determined the Fractional Inhibitory Concentration index (FICI). The FICI is calculated using this formula FIC = [MIC (3HTQ in combination) divided by MIC (3HTQ alone)] + [MIC (thymoquinone in combination) divided by MIC (thymoquinone alone)] + FIC = [MIC (amphotericin B in combination) divided by MIC (amphotericin B alone)]. It involves comparing the MIC of each compound when used in combination with its MIC when used independently. This approach provides a comprehensive assessment of the combined inhibitory effects of the compounds, enabling us to determine whether the interactions are synergistic, additive, or antagonistic.[14,22]

The checkerboard-assay was carefully conducted in triplicate to attain the reliability and reproducibility of the results. The average values obtained from these three independent experiments were noted and analysed for further interpretation.

By employing the checkerboard broth assay, we aimed to gain a deeper understanding of how 3HTQ, THQ, and amphotericin B interact with each other in inhibiting MRSA growth. This methodical approach allowed us to generate robust and reliable data on the potential synergistic effects of these antimicrobial agents, contributing valuable insights to the development of more effective combination therapies versus multidrug-resistant bacterial infections. Every test was performed 3 times to attain the reliability and reproducibility of the results. After conducting the experiments in triplicate, the data from each set of tests were averaged. This process of replication and averaging helps to minimize the impact of any outliers or anomalies in the individual test results, providing a more accurate and representative measure of the true effect or outcome.

Assessment of the Interactions Between the Tested Antimicrobial Agents

To thoroughly investigate the interactions among the 3HTQ, THQ, and amphotericin B under study, we employed a checkerboard assay design. This method allowed us to systematically construct a comprehensive matrix that covered all possible dose combinations of the two drugs within their designated concentration ranges. By doing so, we were able to assess the effects of these combinations on bacterial growth inhibition with a high degree of precision and accuracy.

To quantitatively characterize the interactions between the two drugs, we calculated the Fractional Inhibitory Concentration Index (FICI). The FICI provides a numerical value that helps interpret the nature of the drug interactions. According to established guidelines, the interpretation of FICI results is as follows:

- **FICI ≤ 0.5**: This value indicates a synergistic interaction between the drugs, meaning that the combined effect is significantly greater than the sum of their individual effects. In practical terms, this corresponds to a reduction of at least two dilution steps in the MIC of each drug when used together.
- **0.5 < FICI ≤ 1**: Values within this range signify an additive effect, where the combined effect is roughly equal to the sum of the individual effects of the drugs.
- **1 < FICI ≤ 2**: These values suggest indifference, indicating that the combined effect is neither significantly greater nor less than the sum of the individual effects.
- **FICI > 2**: Values exceeding 2 indicate antagonism, where the combined effect is less effective than the individual effects of the drugs, suggesting that the drugs interfere with each other's activity.

The checkerboard assay was performed meticulously, with each combination being tested in triplicate to ensure the reliability and reproducibility of the results. The average FICI values were then calculated and recorded for subsequent analysis.

By employing this detailed and systematic approach, we aimed to gain a comprehensive understanding of how the antimicrobial agents interact with each other. This information is crucial for developing effective combination therapies, especially in the context of treating multidrug-resistant bacterial infections. The data obtained from this study provide valuable insights into the potential synergistic, additive, indifferent, or antagonistic relationships between the tested drugs, guiding future research and clinical applications.

In silico Analysis

To study the synergetic effect of the triple compounds, we used molecular docking and molecular dynamic simulations (MD simulation). The ligands were obtained from the PubChem database and prepared for docking using LigPrep in the Maestro tool (version 2020). The preparation steps include the addition of hydrogen, protonation, and energy minimization. An essential protein of Methicillin-Resistant *S. aureus* (PBP2a) which is involved in the resistance to beta-lactam antibiotics, was selected for in silico study. The crystal structure of the protein was obtained from PDB database. The protein was prepared for docking, and then active site and allosteric sites were determined according to previous publications.[23,24]

To study the stability of the generated complex we employed the molecular dynamics (MD) simulations using the Desmond module within the Schrödinger Maestro suite (version 2020). The protein-ligand complexes were solvated in an orthorhombic box with a 10 Å buffer using the TIP4P water model. Counterions (Na^+/Cl^-) were added to neutralize the system and maintain an ionic strength of 0.15 M. The system was first minimized using the OPLS3e force field, followed by two equilibration steps: NVT ensemble (constant Number, Volume, Temperature) for 1 ns to stabilize the temperature at 300 K using the Nose–Hoover thermostat. NPT ensemble (constant Number, Pressure, Temperature) for another 1 ns at 1 atm pressure.

As a first screening step, a 50 ns simulation of the ligand–protein interaction was conducted, although longer simulations (100–500 ns) are commonly applied for more comprehensive computations. The production MD run was conducted for 50 ns with a time step of 2 fs. Periodic boundary conditions were applied in all three dimensions, and the Particle Mesh Ewald (PME) method was used to calculate long-range electrostatics. The trajectories were saved every 100 ps and were used as input for principal component analysis (PCA). VMD software[25] was used to generate.dcd files from MD simulation trajectories, which were then used as input for PCA analysis using the Bio3D package.[26]

Statistical Analysis

The data obtained from the experiments were analyzed using GraphPad Prism version 8. To compare the antibacterial efficacy between monotherapy and combination therapy, an unpaired *t*-test was performed. An unpaired *t*-test was used to

compare the effects of monotherapy and triple-combination treatment by grouping each condition as a single outcome. The checkerboard design was used to evaluate the general difference between the two treatment strategies rather than multiple pairwise comparisons. This statistical test was chosen to determine whether there was a significant difference between the means of the two groups. A p-value of less than 0.05 was considered statistically significant, indicating that the observed differences were unlikely to have occurred due to random variation. This approach ensured the reliability and accuracy of the statistical comparisons conducted in this study.

Results

MIC Values of THQ, 3HTQ, and Amphotericin B

Before implementing the checkerboard-assay, it is essential to assess the minimum inhibitory concentrations (MICs) of 3HTQ, amphotericin B, and THQ. This step is crucial for ensuring accurate and reliable results. The MIC is defined as the lowest concentration of the compound that fully inhibits visible growth of the organism after overnight incubation. The MIC values for THQ, as presented in Table 1, range from 8 to 64 µg/mL. For 3HTQ, the MIC value is consistently 32 µg/mL, whereas amphotericin B exhibits MIC values varying from 16 to 64 µg/mL (Table 1). With these MIC results, we meticulously designed a checkerboard assay. This assay involved mixing different concentrations of thymoquinone and 3HTQ to investigate their combined effects. The experimental design was structured to evaluate the potential synergistic or additive interactions between these compounds, particularly against resistant MRSA strains. The detailed MIC data and the subsequent checkerboard-assay are integral to understanding the interactions between THQ, 3HTQ,

Table 1 The MICs Interpretation of 3HTQ, Amphotericin B, and THQ

Number of Strains	MIC of 3-Hydrazinoquinoxaline-2-Thiol (µg/mL)	MIC of Amphotericin B (µg/mL)	MIC of Thymoquinone (µg/mL)
1 MRSA 72	32	64	32
2 MRSA 73	32	32	16
3 MRSA 101	32	32	16
4 MRSA 102	32	16	32
5 MRSA 104	32	16	32
6 MRSA 98	32	64	32
7 MRSA 107	32	64	64
8 MRSA 106	32	32	32
9 MRSA 93	32	64	16
10 MRSA 95	32	16	64
11 MRSA 80	32	32	32
12 MRSA 90	32	64	64
13 MRSA 105	32	32	32
14 MRSA 91	32	64	32
15 MRSA 92	32	64	32
16 MRSA 70	32	64	32
17 MRSA 75	32	64	8
18 MRSA 100	32	64	32

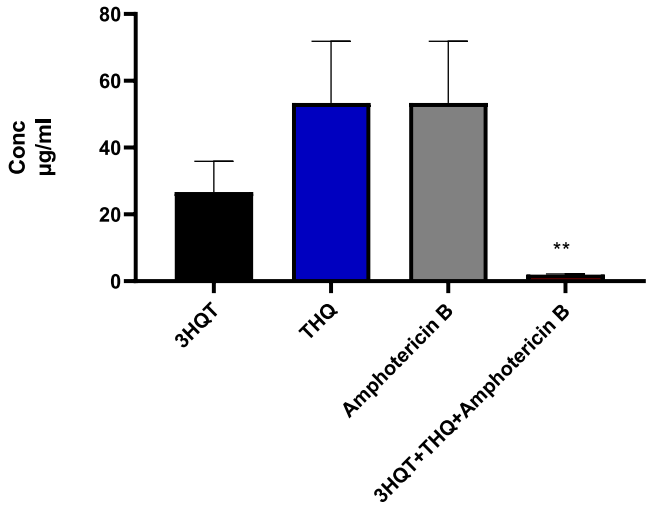

Figure 1 MIC reductions observed with thymoquinone (THQ), 3-hydrazinoquinoxaline-2-thiol (3HTQ), and amphotericin B, alone and in combination. The y-axis represents compound concentrations (µg/mL). Combination therapy produced up to 32-fold MIC decreases (MRSA 107). Statistical analysis (*t*-test) showed significant differences between monotherapy and combination therapy (**p = 0.0098), highlighting the enhanced effect of the combinations.

and amphotericin B. These findings will contribute significantly to the development of more effective treatments for infections caused by resistant MRSA strains and various clinical MRSA species.

In our study, we conducted a checkerboard test to evaluate how the combination of 3HTQ, amphotericin B and THQ affects various clinical strains of MRSA. Initially, we found that amphotericin B alone was ineffective in inhibiting MRSA growth, which was consistent across individual applications of each drug. However, a significant finding emerged when thymoquinone was combined with both 3HTQ and amphotericin B. We noticed a remarkable reduction in the MICs of THQ, with reductions of up to 32-fold in certain strains. Similarly, when 3HTQ and amphotericin B were paired with THQ, significant decreases in their MICs were noted, also reaching reductions of up to 32-fold in specific strains. Of note, once 3HTQ and THQ were added to amphotericin B, huge decreases in their MICs were noted, also reaching reductions of up to 32-fold in different species (Figure 1).

Furthermore, our study revealed that combining thymoquinone, 3HTQ, and amphotericin B led to even greater reductions in MICs, specifically by 4-fold and 16-fold versus certain MRSA strains. This substantial decrease in MICs underscores the enhanced efficacy of the combination therapy, as detailed in Table 2 and illustrated in Figure 2 of our findings. 100% synergy was noticed when we employed the combination of THQ, 3HTQ, and amphotericin B against 18 different MRSA clinical strains. Suggesting that the triple antibiotic combination produces synergistic effect against different clinical MRSA strains (Table 2 and Figure 2).

Table 2 FIC and FICI of 3HTQ, Amphotericin B, and THQ

Number of Strains	FIC of 3-Hydrazinoquinoxaline-2-Thiol	FIC of Amphotericin B	FIC of Thymoquinone	FICI	Interpretation
1 MRSA 72	0.04	0.041	0.057	0.138	Synergy
2 MRSA 73	0.093	0.061	0.067	0.221	Synergy
3 MRSA 101	0.06	0.168	0.057	0.285	Synergy
4 MRSA 102	0.033	0.061	0.04	0.134	Synergy
5 MRSA 104	0.08	0.074	0.081	0.235	Synergy
6 MRSA 98	0.067	0.068	0.067	0.202	Synergy

(*Continued*)

Table 2 (Continued).

Number of Strains	FIC of 3-Hydrazinoquinoxaline-2-Thiol	FIC of Amphotericin B	FIC of Thymoquinone	FICI	Interpretation
7 MRSA 107	0.06	0.038	0.031	0.129	Synergy
8 MRSA 106	0.08	0.172	0.047	0.299	Synergy
9 MRSA 93	0.096	0.266	0.082	0.444	Synergy
10 MRSA 95	0.107	0.095	0.053	0.255	Synergy
11 MRSA 80	0.083	0.041	0.186	0.31	Synergy
12 MRSA 90	0.109	0.023	0.048	0.18	Synergy
13 MRSA 105	0.088	0.059	0.061	0.208	Synergy
14 MRSA 91	0.137	0.058	0.075	0.27	Synergy
15 MRSA 92	0.083	0.034	0.091	0.188	Synergy
16 MRSA 70	0.109	0.057	0.067	0.233	Synergy
17 MRSA 75	0.136	0.141	0.083	0.36	Synergy
18 MRSA 100	0.136	0.061	0.081	0.278	Synergy

Notes: Fractional Inhibitory Concentration (FIC) and Fractional Inhibitory Concentration Index (FICI) of 3HTQ, Amphotericin B, and THQ combinations against tested microbial strains. FIC values were calculated by dividing the MIC of each drug in combination by its MIC alone.

Molecular Docking

A molecular docking study was performed to explore the possible binding conformations and interactions of the tested ligands with the target protein. To evaluate the reliability of the docking protocol, the co-crystallized ligand Penicillin G was redocked into the active site of penicillin-binding protein 2a (PBP2a). The redocking reproduced the ligand pose with an RMSD of 2.8 Å between the docked and crystallographic conformations (Figure 3), indicating a reasonable, though not optimal, reproduction of the binding mode. All ligands were subsequently docked into both the active and allosteric sites of the PBP2a protein. The docking scores of the ligands are summarized in Table 3. The XP scores were −3.8 kcal/mol for thymoquinone and −4.1 kcal/mol for 3-Hydrazinoquinoxaline-2-thiol, while amphotericin B showed the lowest docking score (−6 kcal/mol), suggesting a potentially stronger predicted interaction with the target site (Figure 4).

MD Simulation

The MD simulation was utilised to evaluate the stability of the generated complex formed from the interaction of three ligands—thymoquinone, 3-Hydrazinoquinoxaline-2-Thiol, and amphotericin B—with the PBP2a protein of methicillin-resistant *S. aureus* (MRSA). This approach is particularly relevant for combating pathogenic infections caused by β-lactam-resistant microbial strains, as the ligands showed potential binding interactions with the PBP2a protein at both the active and allosteric sites. The RMSD plot provides insight into the structural stability of the protein–ligand complexes during the simulation when interacting with the target protein. The RMSD in Figure 5A and B), shows the interaction between thymoquinone and PBP2a, in which protein's RMSD stabilizes following an initial period of fluctuation, suggesting that the protein structure suggesting that the protein structure remains relatively stable during the interaction. Throughout the simulation, the ligand represented by the red line also shows higher fluctuation in range of 1.4 To 5.4Å. This suggests that thymoquinone may undergo conformational adjustments within the PBP2a binding pocket. Meanwhile, the ligand 3-Hydrazinoquinoxaline-2-Thiol showed an early period of adjustment, and the RMSD of the PBP2a protein stabilizes, demonstrating structural stability. Throughout the simulation time, the ligand's RMSD showed

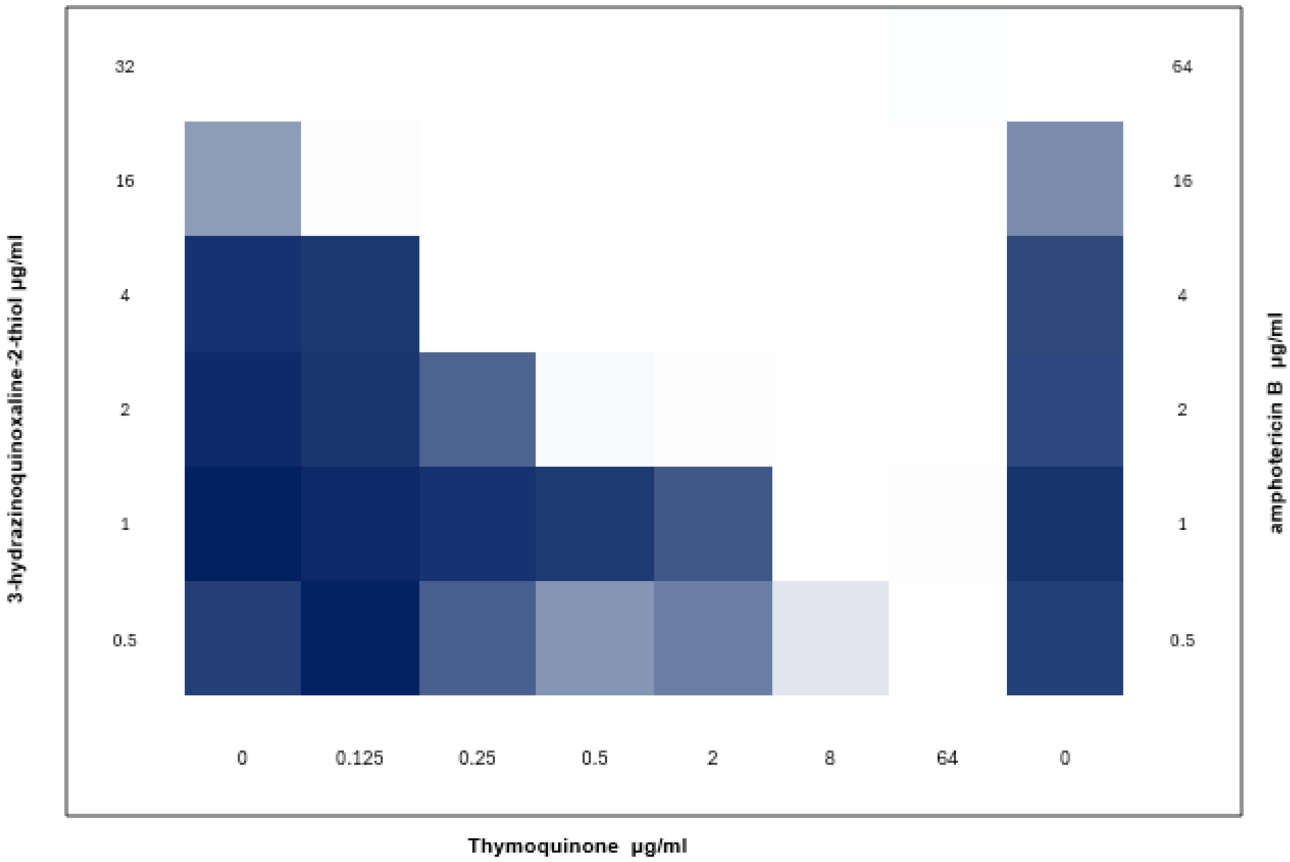

Figure 2 Checkerboard Assay of MRSA 107 Clinical Strain with 3HTQ, Amphotericin B, and THQ. This figure shows the combined effects of 3HTQ, Amphotericin B, and THQ against MRSA 107. Drug concentrations are arranged along the axes, with white cells indicating no bacterial growth (inhibition) and dark cells indicating growth. The figure highlights the synergistic interactions among the three agents.

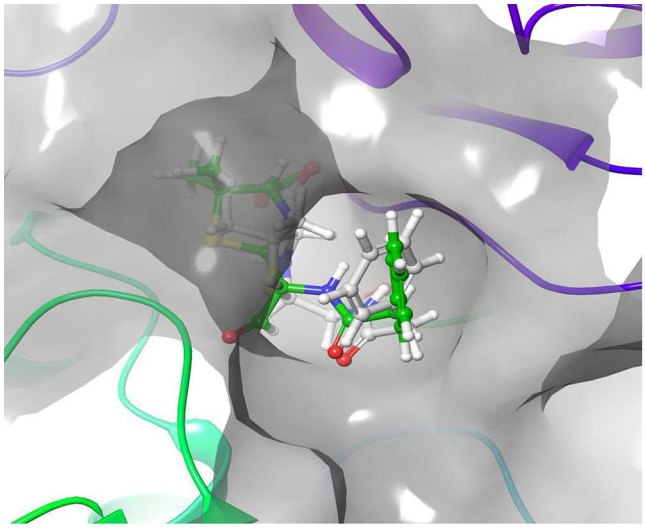

Figure 3 Redocking of the co-crystallized ligand Penicillin G within the active site of penicillin-binding protein 2a (PBP2a) from methicillin-resistant *Staphylococcus aureus* (MRSA) strain 27r. The figure displays both the original ligand conformation (in green) extracted from the crystal structure and the redocked conformation (in white) predicted via molecular docking. Penicillin G, a β-lactam antibiotic, contains a fused β-lactam and thiazolidine ring core, a carboxylic acid group, and a benzyl side chain, all of which contribute to its binding affinity. The active site cavity is shown as a semi-transparent surface, with protein secondary structures illustrated as colored ribbons (cyan and purple). The docking protocol successfully re-positioned the ligand within the binding pocket, achieving an RMSD of 2.8 Å between the docked and crystallographic poses. This RMSD indicates a moderate agreement and confirms that the docked ligand adopts a similar overall orientation, with some variation in side-chain positioning—especially in the benzyl group—likely due to conformational flexibility.

https://doi.org/10.2147/IJGM.S603479

Table 3 Docking Scores of the Ligands and Protein PBP2a

Compound	PubChem ID	XP score	Protein RMSD	Ligand RMSD
Thymoquinone	10281	−3.8	2.12 ± 0.35	3.87 ± 0.74
3-hydrazinoquinoxaline-2-thiol	781248	−4.1	1.94 ± 0.28	2.01 ± 0.39
Amphotericin B	5280965	−6	1.66 ± 0.23	1.54 ± 0.21

a lower fluctuation when compared to thymoquinone. The relatively stable RMSD values of both the ligand and protein suggest that the ligand may maintain stable interactions with residues within the active site during the simulation period, these results suggest that the ligand may maintain relatively stable interactions with the active site residues during the simulation period, which may contribute to stable binding within the active site.

3-Hydrazinoquinoxaline-2-Thiol interacts with a stable hydrogen bond with PBP2a MET_372, indicating that this residue plays a crucial role in binding to this ligand (Figure 6A and B). In alignment with our findings, various computational and experimental studies have demonstrated similar interactions of different bioactive molecules with these essential residues (MET_372, Glu239, and Lys148), suggesting their critical role in protein activity.[27–29]

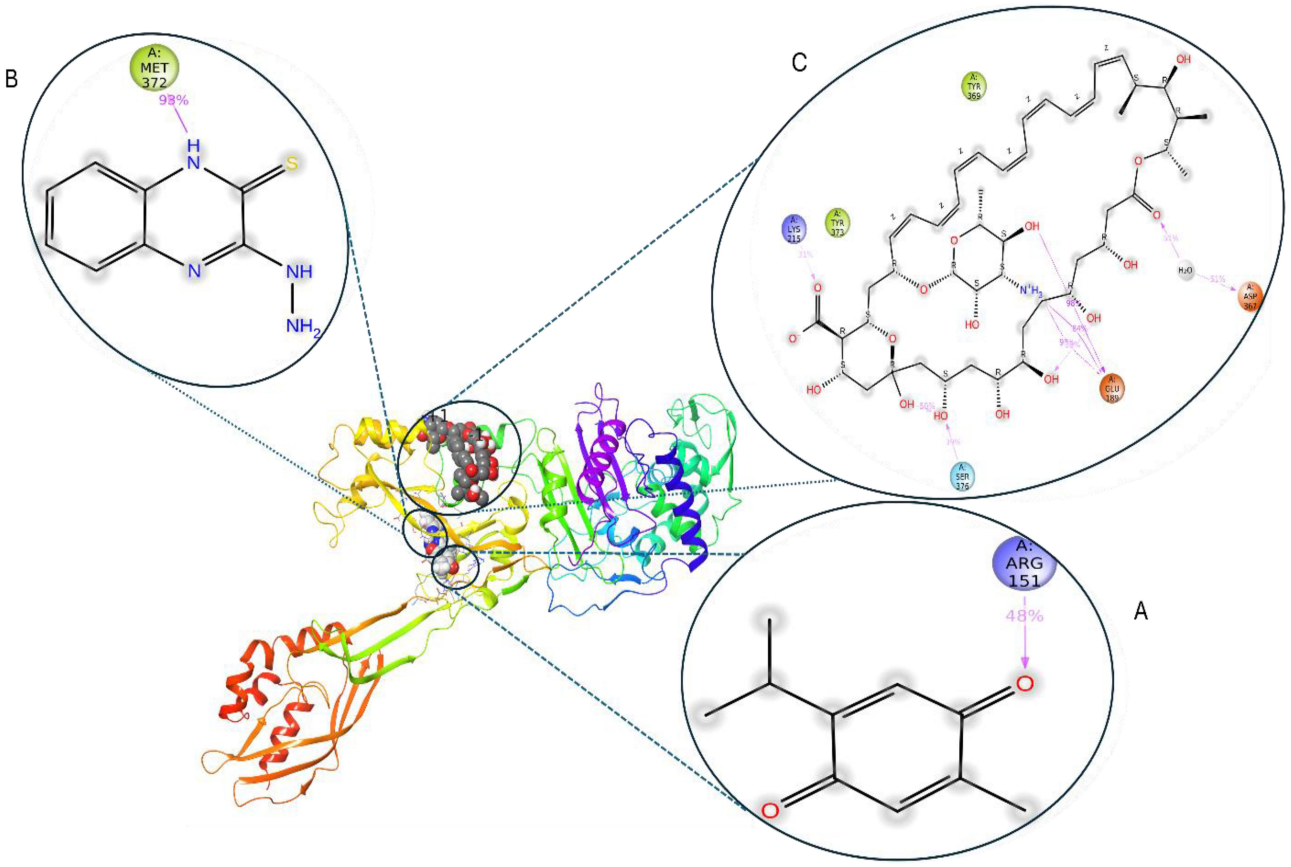

Figure 4 Structural and Interaction Analysis of PBP2a from *S. aureus* with Three Ligands The figure illustrates the 3D structure of Penicillin-Binding Protein 2a (PBP2a) from *Staphylococcus aureus* with ligand interactions highlighted. The main structure is represented as a ribbon diagram, with different domains color-coded for clarity. The ligand binding sites are enlarged for detailed visualization. (**A**) Interaction of Thymoquinone with the active site of PBP2a. The chemical structure of Thymoquinone is shown, highlighting its key interactions with residues in the active site. The interaction with ARG 151 (48% occupancy) suggests a potential role in inhibiting enzymatic function. (**B**) Binding of 3-Hydrazinoquinoxaline-2-Thiol in the active site. The enlarged view displays the interaction of this compound with MET 372 (98% occupancy), indicating strong binding affinity. (**C**) Amphotericin B interacting with the allosteric site of PBP2a. The interaction network, including hydrogen bonding and hydrophobic interactions, is depicted. Residues such as TYR 369, TYR 372, ASP 367, and GLU 189 are involved in stabilizing the ligand in the allosteric pocket.

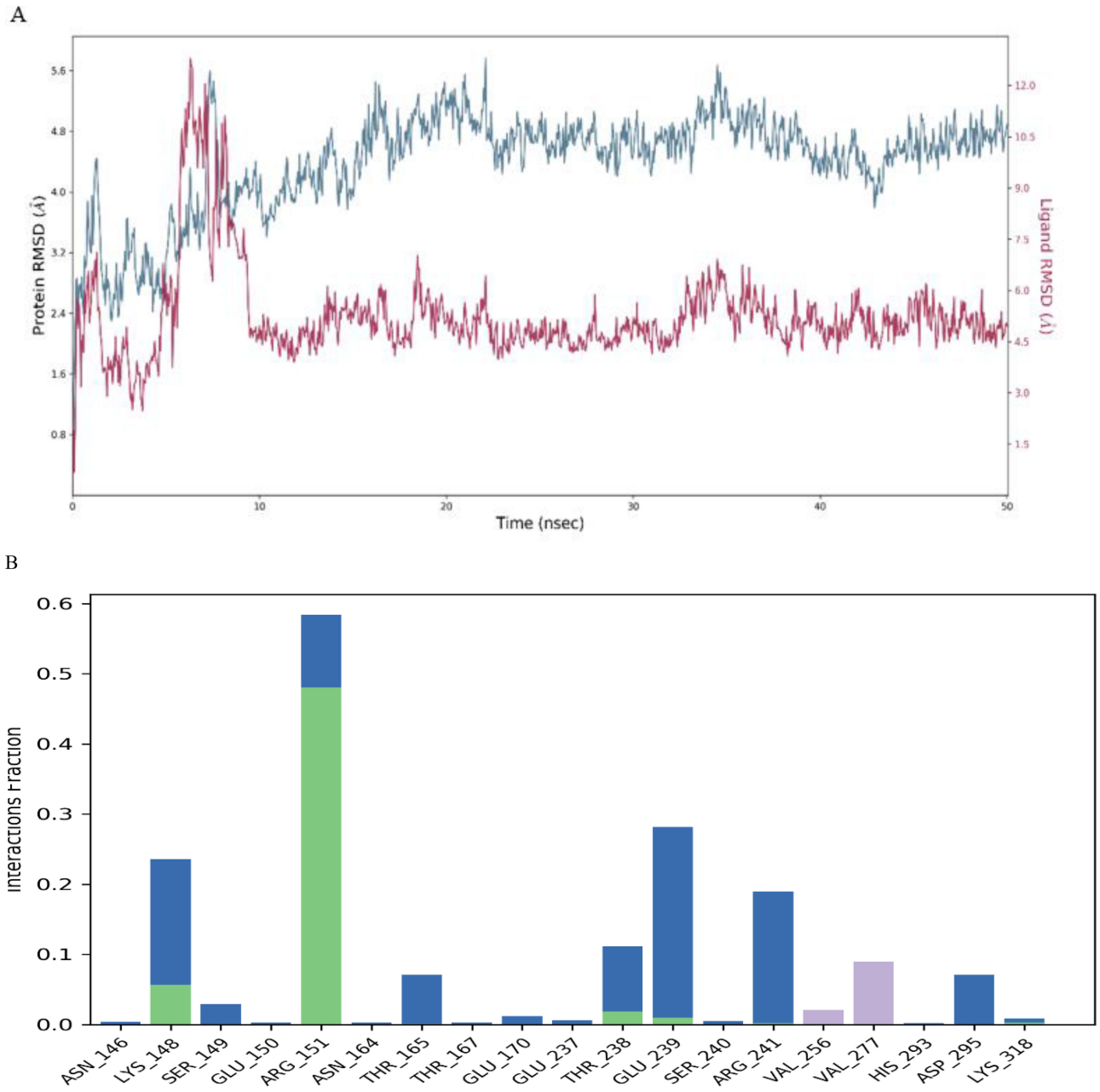

Figure 5 Molecular dynamics (MD) simulation plots depicting the root mean square deviation (RMSD) of Thymoquinone (red) and PBP2a (blue) over time (**A**). The RMSD of PBP2a represents the overall structural stability of the protein, while the RMSD of Thymoquinone indicates the stability of ligand binding within the protein's active site. A lower and more stable RMSD suggests a well-maintained interaction. (**B**) The histogram illustrates the frequency of molecular interactions between Thymoquinone and PBP2a throughout the simulation. Hydrogen bonds (green) contribute to binding specificity and stability, hydrophobic interactions (purple) stabilize the complex by excluding water molecules, and water bridges (blue) mediate indirect interactions through solvent molecules, playing a role in ligand binding dynamics.

Amphotericin B exhibited relatively stable interactions with the protein backbone at the allosteric site and maintains a relatively stable profile throughout the simulation during the whole simulation time, as shown in Figure 7A, the ligand and protein alpha atoms are in contact through most of the simulation period. This stability suggests that amphotericin B may interact favorably with the protein and could potentially influence its activity, although experimental validation is required. Overall, the RMSD profiles suggest that the ligands maintain relatively stable interactions with PBP2a during the simulation period, supporting the docking observations. Notably, Amphotericin B exhibited the most stable interaction profile with the lowest RMSD fluctuations, while Thymoquinone showed greater conformational variability during the simulation, which may indicate a more flexible binding mode (Table 3).

https://doi.org/10.2147/IJGM.S603479

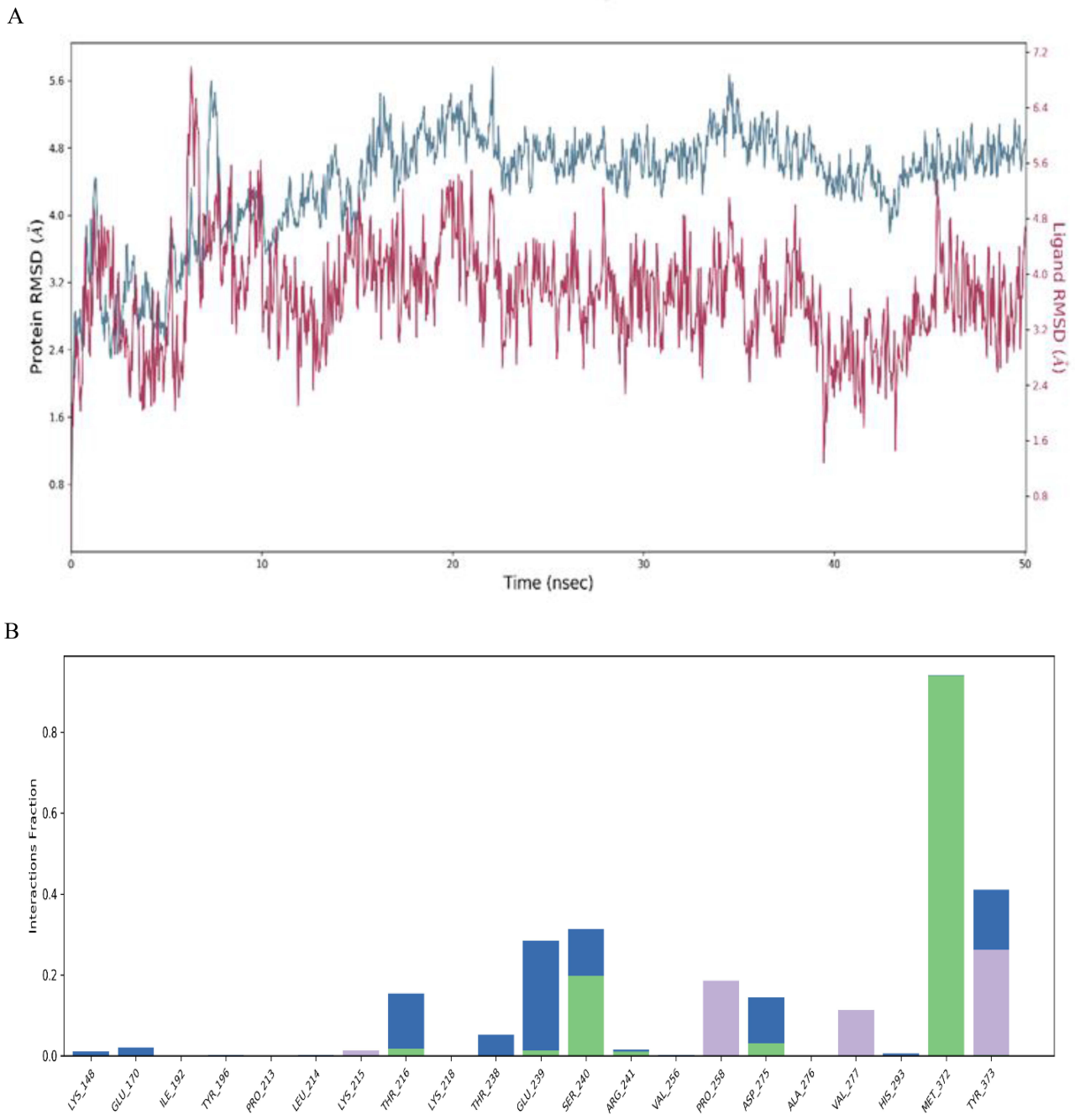

Figure 6 Molecular dynamics (MD) simulation plots depicting the root mean square deviation (RMSD) of 3-Hydrazinoquinoxaline-2-Thiol (red) and PBP2a (blue) over time (**A**). The RMSD of PBP2a represents the overall structural stability of the protein, while the RMSD of 3-Hydrazinoquinoxaline-2-Thiol indicates the stability of ligand binding within the protein's active site. A lower and more stable RMSD suggests a well-maintained interaction. (**B**) The histogram illustrates the frequency of molecular interactions between 3-Hydrazinoquinoxaline-2-Thiol and PBP2a throughout the simulation. Hydrogen bonds (green) contribute to binding specificity and stability, hydrophobic interactions (purple) stabilize the complex by excluding water molecules, and water bridges (blue) mediate indirect interactions through solvent molecules, playing a role in ligand binding dynamics.

More details about the interaction of the compounds with protein residues is shown in histograms (Figure 7B), thymoquinone interaction with protein forms significant contacts with several residues, most notably ARG_151, which shows a stable hydrogen bond, suggesting a strong stability with the protein active site. Other residues such as GLU_239, LYS_148, and VAL_256 also show notable water bridges shown in blue color (Figure 5B). Amphotericin B exhibits a more diverse interaction profile, with significant contacts with several residues including GLU_189, LYS_215, and

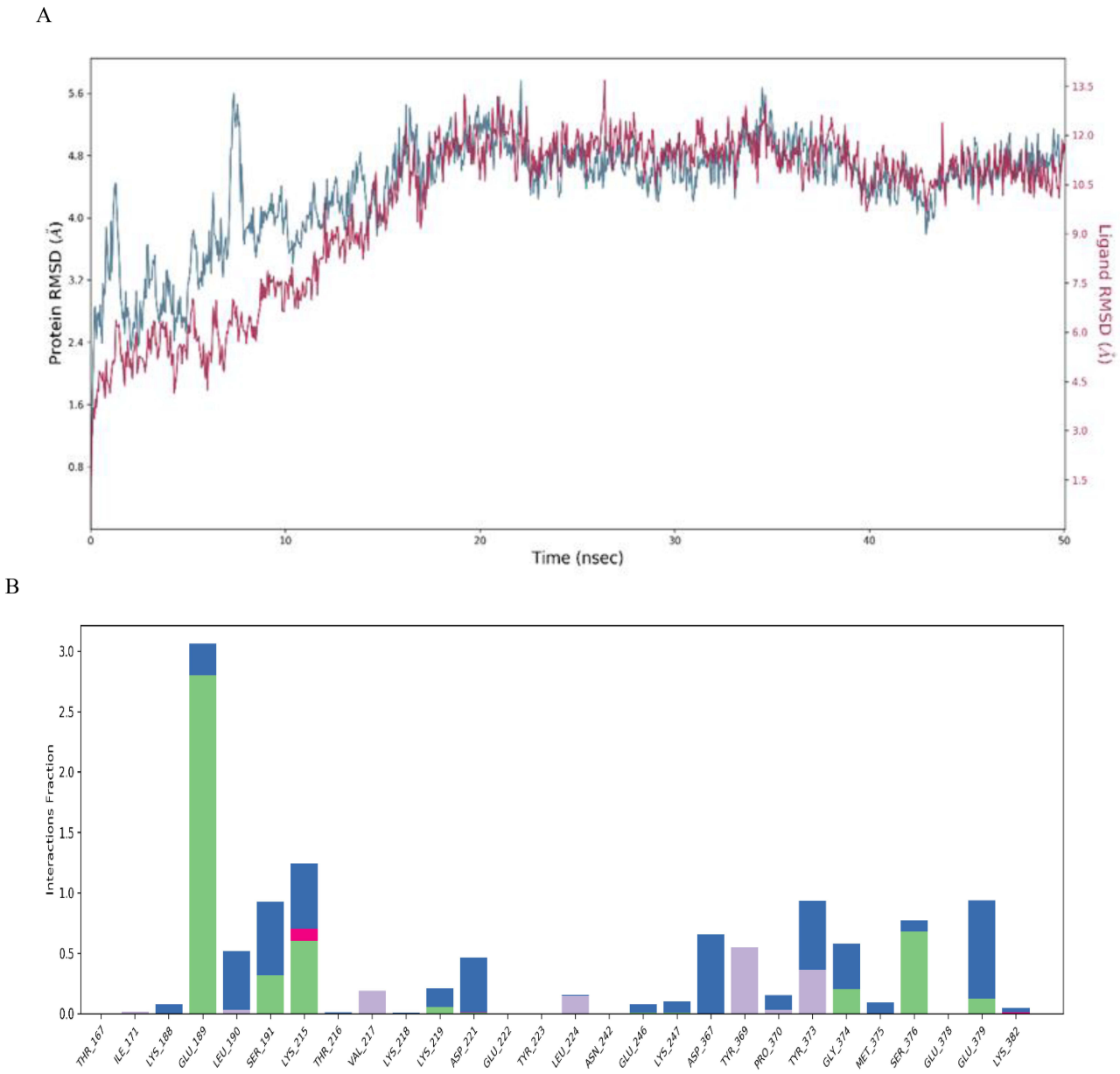

Figure 7 Molecular dynamics (MD) simulation plots depicting the root mean square deviation (RMSD) of Amphotericin B (red) and PBP2a (blue) over time (**A**). The RMSD of PBP2a represents the overall structural stability of the protein, while the RMSD of Amphotericin B indicates the stability of ligand binding within the protein's active site. A lower and more stable RMSD suggests a well-maintained interaction. (**B**) The histogram illustrates the frequency of molecular interactions between Amphotericin B and PBP2a throughout the simulation. Hydrogen bonds (green) contribute to binding specificity and stability, hydrophobic interactions (purple) stabilize the complex by excluding water molecules, and water bridges (blue) mediate indirect interactions through solvent molecules, playing a role in ligand binding dynamics.

SER_376. Those high numbers of stable hydrogen (green), hydrophobic (purple) and water bridge bonds (blue) could have contributed to amphotericin B significantly higher binding stability during MD simulation. Residue SER_376 is considered among the most important catalytic residues in the allosteric site of this protein.[30]

Principal Component Analysis (PCA)

PCA and RMSF analyses were performed to evaluate the dynamic behaviour of the PBP2a protein in complex with the ligands during MD simulations.[30] As shown in Figure 8A, the first principal component (PC1) accounts for the highest proportion of variance (38.93%), followed by PC2 (13.68%) and PC3 (11.99%). The PCA plots show clusters representing sampled conformational states of the protein-ligand complexes over the 50 ns simulation. The dispersion

https://doi.org/10.2147/IJGM.S603479

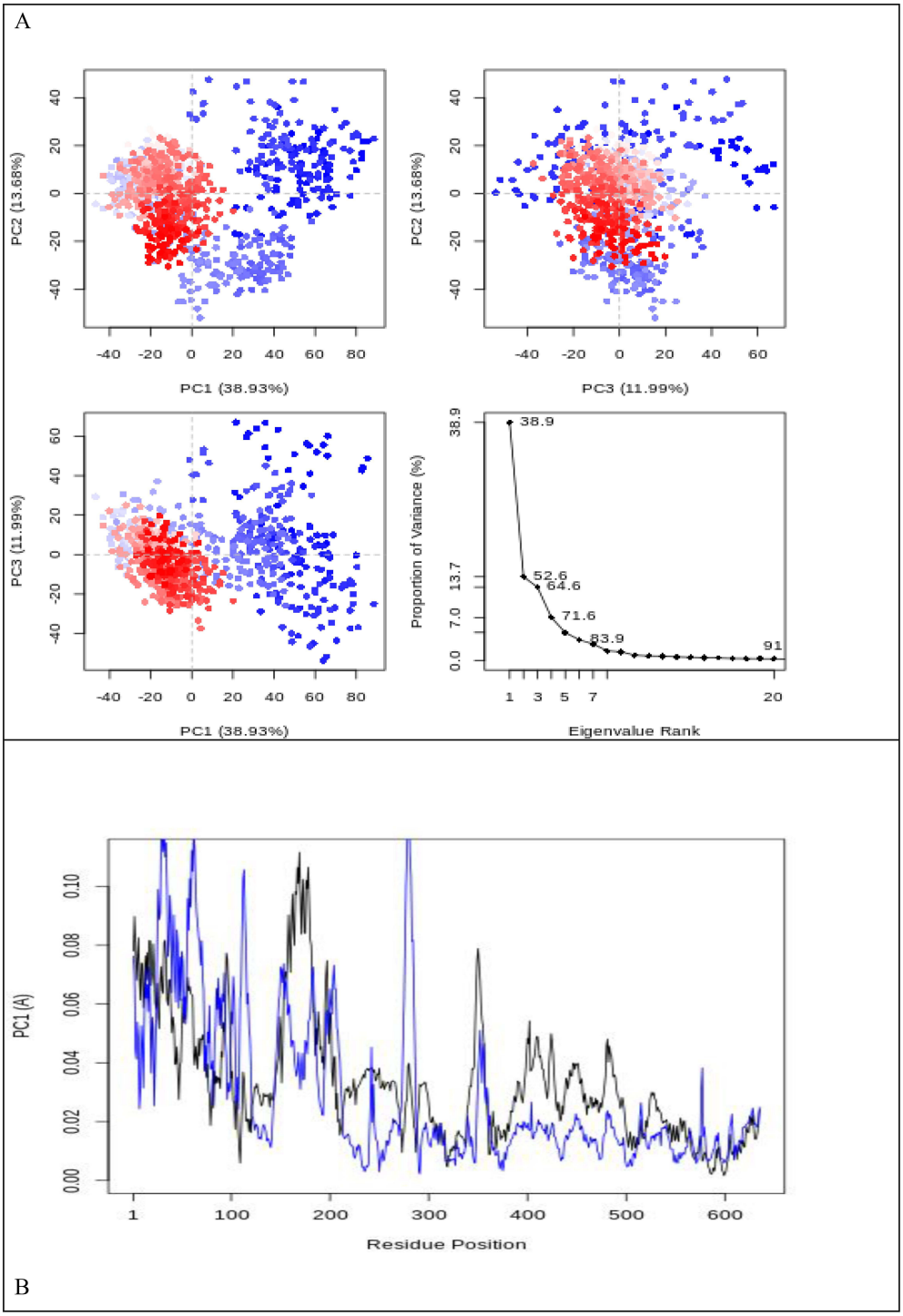

Figure 8 Principal Component Analysis (PCA) and Root Mean Square Fluctuation (RMSF) Analysis of the Protein-Ligand Complex (**A**) PCA of the protein-ligand complex. The plot represents the projection of the molecular dynamics (MD) trajectory onto the first three principal components (PC1, PC2, and PC3). Each point corresponds to a conformational state of the complex sampled during the simulation. The color gradient from red to blue represents different time points along the trajectory, with red indicating the initial frames and blue representing the later frames. The eigenvalues associated with the first three principal components suggest that PC1 captures the largest variance (38.93%), followed by PC2 (13.68%) and PC3 (11.99%). The scree plot in the bottom right corner illustrates the proportion of variance explained by each eigenvalue, highlighting the dominance of the first few principal components. (**B**) Root Mean Square Fluctuation (RMSF) along the first principal component (PC1). The plot represents the RMSF values of individual residues along the PC1 eigenvector, showing fluctuations in atomic positions during the MD simulation. The black and blue lines correspond to different states or conditions of the protein-ligand complex. Higher RMSF values indicate regions of increased flexibility, while lower values suggest more stable regions. The fluctuations are more pronounced in the N-terminal and loop regions, while the core and secondary structure elements exhibit relatively lower mobility.

of clusters, particularly along PC1, suggests that distinct conformational states of the protein may be stabilized by each ligand, which may influence ligand binding dynamics and should be further investigated experimentally.[31]

RMSF analysis provides residue-level flexibility along PC1, with different protein-ligand states indicated by black and blue lines. High RMSF values correspond to flexible regions, while lower values correspond to more rigid regions.[32] Increased flexibility was observed in the N-terminal and some loop regions, whereas the protein core remained more stable In the ligand-binding region (residues 200–350), overall lower fluctuations were observed, suggesting that different ligands may modulate local protein flexibility, which could be relevant to their interaction dynamics and should be further investigated experimentally (Figure 8B).

Discussion

MRSA strains showed varying resistance profiles to thymoquinone (THQ), 3-hydrazinoquinoxaline-2-thiol (3HTQ), and amphotericin B in the study. However, when combined with 3HTQ or amphotericin B, THQ's antimicrobial activity was markedly enhanced, resulting in significant reductions in MIC values. There was a significant improvement in efficacy with the triple combination, suggesting that simultaneous targeting of multiple bacterial pathways may enhance antibacterial activity.

The observed reductions in MIC values when using combination therapies have significant clinical implications. The ability to lower MICs suggests that lower doses of each agent can be used, potentially reducing the risk of adverse effects and toxicity associated with higher doses of individual drugs.[14] Furthermore, the synergistic effects observed in our study provide a strong rationale for further investigation into combination therapies as a viable strategy to combat multidrug-resistant MRSA infections.

Our research highlights the synergistic effects of combining 3HTQ and thymoquinone on various clinical strains of Methicillin-resistant *S. aureus* (MRSA). The observed synergy can be attributed to multiple mechanisms comprising of the inhibition of distinct signalling pathways. THQ acts its antimicrobial action primarily by producing unreversible harm to bacterial morphology, which includes compromising cell membrane integrity, leading to protein leakage, and disrupting intracellular proteins.[33–35] This multifaceted attack disrupts the bacterial cell's structural and functional integrity. Conversely, 3HTQ has been demonstrated to play a crucial role in inhibiting DNA synthesis. By impeding DNA synthesis, 3HTQ adds an additional layer of effectiveness in controlling the proliferation and survival of MRSA strains.[36–38]

In addition, the combined action of thymoquinone and 3HTQ against diverse MRSA strains may be attributed to the generation of reactive oxygen species (ROS). Increasing ROS levels can disrupt electron transport chains, cause oxidative stress, and ultimately lead to bacterial cell death. It has been suggested that thymoquinone may contribute to its antimicrobial activity by encouraging ROS formation. The synergistic effects of 3HTQ and thymoquinone on MRSA strains could partly be explained by the combined effect of ROS generation and their distinct mechanisms.[39–41] While these mechanisms are inferred from previous literature, the present study did not include molecular assays to directly confirm ROS generation, DNA synthesis inhibition, or membrane disruption. Therefore, these explanations remain hypothetical and require further experimental testing.

It has been demonstrated that the anti-bacterial possibility of amphotericin B was detected via antimicrobial screening, molecular docking analysis, and structural dynamics evaluations using molecular dynamics simulations. The antimicrobial screening demonstrated considerable anti-bacterial activity of amphotericin B, with a MIC of 16 µg/mL and a minimum bactericidal concentration (MBC) of 32 µg/mL. Molecular docking suggested potential interactions of amphotericin B with the target protein, particularly at both the active and allosteric sites, which may contribute to its observed in vitro activity, interacting effectively with both the active site, the C-terminal, and non-penicillin binding regions.[19] MD simulations revealed the extraordinary stability of the amphotericin B -protein complex. Notably, amphotericin B showed the ability to bind to both the C-terminal active site domain and non-penicillin binding domain, which are crucial for allosteric regulation.[19] Our results are in agreement with the previous study.[36] The computational findings may explain the observed in vitro activity, but in silico predictions should be interpreted cautiously, as they do not necessarily confirm direct biological target engagement.

Amphotericin B can be considered a strong anti-bacterial drug for combating pathogenic infections, particularly those caused by β-lactam-resistant microbial strains as it shows strong binding to the PBP2a protein at both active sites and allosteric regions. Additionally, we assessed hydrogen bond formation during the simulations to better understand the stability and interaction dynamics of the complexes. The molecular docking study provided valuable insights into the potential interactions between three ligands—thymoquinone, 3-Hydrazinoquinoxaline-2-Thiol, and amphotericin B and the PBP2a protein of Methicillin-Resistant *S. aureus* (MRSA). The docking scores revealed that amphotericin B exhibited the most favourable binding affinity with a docking score of −6 kcal/mol, compared to −3.8 and −4.1 kcal/mol for thymoquinone and 3-Hydrazinoquinoxaline-2-Thiol, respectively. These results suggest that amphotericin B has a higher potential for interacting effectively with the PBP2a protein, possibly due to its ability to establish more stable and significant contacts at the allosteric site.

The MD simulation provided further insights into the stability and binding dynamics of these ligands with PBP2a. The RMSD analysis indicated that all three ligands interacted differently with the protein. Thymoquinone showed substantial fluctuations, suggesting conformational changes when binding to the active site, while 3-Hydrazinoquinoxaline-2-Thiol exhibited more stability, implying a consistent interaction with the protein's active site. MD simulations indicated relatively stable interactions of amphotericin B with the protein, particularly at the allosteric site, which could support its potential inhibitory activity, though experimental validation is needed. The stable interaction patterns observed in amphotericin B could serve as a robust inhibitor of PBP2a, thus offering a promising approach for combating MRSA infections. Although amphotericin B was traditionally classified as an antifungal, our in vitro and in silico studies suggest it may have antibacterial activity; however, further mechanistic and experimental studies are needed to confirm its potential.

Detailed residue interaction analysis revealed that thymoquinone, 3-Hydrazinoquinoxaline-2-Thiol, and amphotericin B formed significant contacts with crucial residues in PBP2a. For instance, thymoquinone's stable hydrogen bond with ARG_151 and water bridges with residues like GLU_239 and LYS_148 suggest a strong binding affinity to the protein's active site. Similarly, 3-Hydrazinoquinoxaline-2-Thiol's interaction with MET_372 highlighted its potential for stable binding. Amphotericin B exhibited a diverse interaction profile, forming multiple stable hydrogen, hydrophobic, and water bridge bonds with residues like GLU_189, LYS_215, and SER_376, which may have contributed to its superior binding stability during the MD simulation.

The Principal Component Analysis (PCA) and Root Mean Square Fluctuation (RMSF) plots offered additional insights into the dynamic behaviour of the PBP2a protein in complex with these ligands. The PCA revealed distinct clusters representing various protein-ligand conformations, with significant variance along PC1, indicating that each ligand might stabilize different conformational states of the protein, which could influence their inhibitory mechanisms. The RMSF analysis showed that the regions where ligands bind (residues 200 to 350) exhibited higher stability, indicating that ligand binding could significantly affect the flexibility and rigidity of specific protein regions. Computational analyses, including docking and MD simulations, suggest that amphotericin B may interact more stably with PBP2a compared to thymoquinone and 3-Hydrazinoquinoxaline-2-Thiol. These findings complement the observed in vitro synergy, providing mechanistic hypotheses that warrant further experimental validation. These findings pave the way for further experimental validation and development of these compounds as effective treatments against MRSA.

One of the limitations of this study is that the hypothesized mechanism of action for the observed synergy between 3-Hydrazinoquinoxaline-2-Thiol, thymoquinone and amphotericin B was based primarily on speculation and literature-derived insights, rather than direct experimental validation. While we have proposed potential mechanisms, such as the involvement of reactive oxygen species (ROS) generation or DNA synthesis inhibition, these remain speculative without experimental confirmation. Future studies that incorporate experimental validation, such as ROS quantification and DNA synthesis inhibition assays, will be necessary to better understand the underlying synergistic mechanisms. Another limitation of this study is that the discussion extrapolates the findings to potential clinical applications without sufficient supporting in vivo or clinical trial data. While we have highlighted the promising in vitro results, we acknowledge that the lack of in vivo studies or clinical trials limits the direct applicability of our findings to clinical practice. Additionally, there is a limitation to this study in that the observed reductions in MIC values were obtained under in vitro conditions, which may not be directly applicable to clinically achievable drug concentrations or pharmacokinetic profiles. It should

be noted that the molecular docking and molecular dynamics simulation performed for this study only provide preliminary computational insights into the potential interaction between Amphotericin B and PBP2a. In silico approaches do not fully account for the complex physiological environment of bacterial cells. The dense peptidoglycan wall of MRSA also presents a permeability barrier. Consequently, while the simulations suggest possible binding stability, they do not necessarily confirm physiological target engagement. For these findings to be validated, further experimental studies are needed.

Further research involving in vivo models and clinical trials is essential to validate the therapeutic potential of the combination treatment and to assess its safety and efficacy in human subjects. The present study also lacks a standard reference MRSA strain for comparative analysis. By including an established reference strain, reproducibility could be improved, and previous publications could be compared more easily.

This gap will be addressed in future studies to strengthen the clinical relevance of our findings. While the results demonstrate promising synergistic activity against MRSA, direct extrapolation to clinical applications is limited without pharmacokinetic, pharmacodynamic, and toxicity data.

Biological and clinical feasibility of drug combinations should be evaluated in future studies. The safety profile and therapeutic window of these combinations should be evaluated using in vitro mammalian cytotoxicity assays and in vivo models. At higher concentrations, amphotericin B is known to be toxic. Further pharmacokinetic and pharmacodynamic studies are needed to determine whether synergistic concentrations observed in vitro can be achieved in vivo. This study will clarify the translational potential of these findings and bridge the gap between in vitro observations and clinical applications.

Further investigations, including time-kill kinetics, biofilm assays, and in vivo efficacy and safety models, are essential to assess whether these concentrations can be safely attained in patients. Future work will also include testing against reference MRSA strains to validate the reproducibility and broader applicability of our findings. Moreover, future studies will include the use of scanning electron microscopy to investigate the morphological effects of the triple drug combination on MRSA cell membranes.

Conclusion

Our study has unveiled significant findings regarding the efficacy of THQ, 3HTQ, and amphotericin B against various clinical strains of MRSA. The MICs of these agents demonstrated considerable variability, highlighting the complex resistance mechanisms of MRSA and the potential benefits of combination therapies. Remarkably, when THQ was combined with 3HTQ and amphotericin B, there were significant reductions in MIC values, indicating a synergistic effect. Specifically, the MICs of thymoquinone decreased up to 32-fold in certain strains, and similar reductions were observed for 3HTQ and amphotericin B when combined with THQ. The triple combination showed even greater efficacy, with some strains experiencing up to 16-fold decreases in MICs. This enhanced efficacy may be attributed to the simultaneous targeting of different cellular processes within MRSA bacteria. Potentially, this could reduce resistance development and improve antibacterial activity. By utilizing this synergistic interaction, lower doses of each agent may be used, potentially minimizing adverse effects associated with higher drug concentrations. Combination therapies may be important for treating multidrug-resistant MRSA infections, according to our findings. As a result of the combination of thymoquinone, 3-hydrazinoquinoxaline-2-thiol, and amphotericin B, multiple bacterial pathways may be influenced, enhancing antimicrobial activity. It is possible that these effects are caused by mechanisms such as membrane damage induced by THQ, DNA synthesis inhibition caused by 3HTQ, and possible interactions of amphotericin B with bacterial target proteins. These mechanisms, however, were not directly investigated in the present study and should be considered proposed explanations that require further experimentation. Therefore, future research should identify the precise mechanisms underlying these synergistic effects and evaluate their efficacy and safety in appropriate biological models. It should be noted that the results of this study are based on in vitro experiments and computational analyses. Consequently, further in vivo studies and mechanistic investigations are needed to confirm these combinations' clinical applicability and therapeutic potential.

Acknowledgment

The authors would like to extend their sincere thanks to the Mohamed Saeed Tamer Chair for Pharmaceutical Industries at the Faculty of Pharmacy, King Abdulaziz University (KAU), Jeddah, Saudi Arabia. The support and resources provided by the Chair were instrumental in the successful completion of this research project.

Funding

Open Access publishing is funded by the Deanship of Scientific Research (DSR) at King Abdulaziz University. The authors, therefore, acknowledge the support of DSR with thanks.

Disclosure

The authors declare that they have no conflicts of interest regarding the publication of this manuscript.

References

1. Hu Y, Liu Y, Coates A. Azidothymidine produces synergistic activity in combination with colistin against antibiotic-resistant Enterobacteriaceae. *Antimicrob Agents Chemother*. 2019;63(1):1–11.
2. Kobayashi SD, DeLeo FR. *Staphylococcus aureus* protein A promotes immune suppression. *MBio*. 2013;4(5):4–6. doi:10.1128/mBio.00764-13
3. Ba X, Harrison EM, Lovering AL, et al. Old drugs to treat resistant bugs: methicillin-resistant *Staphylococcus aureus* isolates with mecC are susceptible to a combination of penicillin and clavulanic acid. *Antimicrob Agents Chemother*. 2015;59(12):7396–7404. doi:10.1128/AAC.01469-15
4. Papadimitriou-Olivgeris M, Drougka E, Fligou F, et al. Risk factors for enterococcal infection and colonization by vancomycin-resistant enterococci in critically ill patients. *Infection*. 2014;42(6):1013–1022. doi:10.1007/s15010-014-0678-1
5. Wood SJ, Kuzel TM, Shafikhani SH. Pseudomonas aeruginosa: infections, animal modeling, and therapeutics. *Cells*. 2023;12(1):1–37.
6. Mulani MS, Kamble EE, Kumkar SN, Tawre MS, Pardesi KR. Emerging strategies to combat ESKAPE pathogens in the era of antimicrobial resistance: a review. *Front Microbiol*. 2019;10(4). doi:10.3389/fmicb.2019.00539
7. Ganai AW, Kotwal SK, Wani N, et al. Detection of mecA gene of methicillin resistant *Staphylococcus aureus* by PCR assay from raw milk. *Indian J Anim Sci*. 2016;86(5):508–511. doi:10.56093/ijans.v86i5.58442
8. Ballhausen B, Kriegeskorte A, Schleimer N, Peters G, Becker K. The mecA homolog mecC confers resistance against β-lactams in *Staphylococcus aureus* irrespective of the genetic strain background. *Antimicrob Agents Chemother*. 2014;58(7):3791–3798. doi:10.1128/AAC.02731-13
9. Roemer T, Schneider T, Pinho MG. Auxiliary factors: a chink in the armor of MRSA resistance to b -lactam antibiotics. *Curr Opin Microbiol*. 2013;16(5):538–548. doi:10.1016/j.mib.2013.06.012
10. Bayer AS, Schneider T, Sahl H-G. Mechanisms of daptomycin resistance in *Staphylococcus aureus*: role of the cell membrane and cell wall. *Ann N Y Acad Sci*. 2013;1277(1):139–158. doi:10.1111/j.1749-6632.2012.06819.x
11. Pandey R, Mishra SK, Shrestha A. Characterisation of ESKAPE pathogens with special reference to multidrug resistance and biofilm production in a nepalese hospital. *Infect Drug Resist*. 2021;14(February):2201–2212. doi:10.2147/IDR.S306688
12. Nguyen HM, Graber CJ. Limitations of antibiotic options for invasive infections caused by methicillin-resistant *Staphylococcus aureus*: is combination therapy the answer? *J Antimicrob Chemother*. 2009;65(1):24–36. doi:10.1093/jac/dkp377
13. Swoboda JG, Meredith TC, Campbell J, et al. Discovery of a small molecule that blocks wall teichoic acid biosynthesis in *Staphylococcus aureus*. *ACS Chem Biol*. 2009;4(10):875–883. doi:10.1021/cb900151k
14. Gonzales PR, Pesesky MW, Bouley R, et al. Synergistic, collaterally sensitive β-lactam combinations suppress resistance in MRSA. *Nat Chem Biol*. 2015;11(11):855–861. doi:10.1038/nchembio.1911
15. Meng X-Y, Zhang H-X, Mezei M, Cui M. Molecular docking: a powerful approach for structure-based drug discovery. *Curr Comput Aided Drug Des*. 2011;7(2):146–157. doi:10.2174/157340911795677602
16. Alharbi OS, Alharbi MT, A. Ismail M, et al. Unveiling the synergistic power of 3-hydrazinoquinoxaline-2-thiol and vancomycin against MRSA: an *in vitro* and *in silico* evaluation. *Biomol Biomed*. 2025;25(10):2335–2344. doi:10.17305/bb.2025.11886
17. Elfadil A, Ibrahem K, Abdullah H, Mokhtar JA, Al-Rabia MW, Mohammed HA. Synergistic activity of 3-hydrazinoquinoxaline-2-thiol in combination with penicillin against MRSA. *Infect Drug Resist*. 2024;17(January):355–364. doi:10.2147/IDR.S448843
18. Bazuhair MA, Alsieni M, Abdullah H, et al. The combination of 3-hydrazinoquinoxaline-2-thiol with thymoquinone demonstrates synergistic activity against different candida strains. *Infect Drug Resist*. 2024;17:2289–2298. doi:10.2147/IDR.S464287
19. Farid N, Bux K, Ali K, Bashir A, Tahir R. Repurposing Amphotericin B: anti-microbial, molecular docking and molecular dynamics simulation studies suggest inhibition potential of Amphotericin B against MRSA. *BMC Chem*. 2023;17(1):1–16. doi:10.1186/s13065-023-00980-9
20. Yan X, Zheng W, Xu F-S. Evaluation of the antibacterial activity of 3-hydrazinoquinoxaline-2-thiol compound against extended-spectrum beta-lactamases producing bacteria. *Eur Rev Med Pharmacol Sci*. 2024;28(10):2024. doi:10.26355/eurrev_202403_35617
21. Elfadil A, Alzahrani AM, Abdullah H, et al. Evaluation of the Antibacterial Activity of Quinoxaline Derivative Compound Against Methicillin-Resistant *Staphylococcus aureus*. *Infect Drug Resist*. 2023;16:2291–2296. doi:10.2147/IDR.S401371
22. Ibrahem K, Alhazmi W, Niyazi HA, et al. An In vitro investigation of the potential synergistic effect of 3-hydrazinoquinoxaline-2-thiol and thymoquinone's against methicillin resistant *Staphylococcus aureus* (MRSA). *J Pure Appl Microbiol*. 2024;18(4):2837–2849. doi:10.22207/JPAM.18.4.55
23. Chiang YC, Wong MTY, Essex JW. Molecular dynamics simulations of antibiotic ceftaroline at the allosteric site of penicillin-binding protein 2a (PBP2a). *Isr J Chem*. 2020;60(7):754–763. doi:10.1002/ijch.202000012
24. Alhadrami HA, Hamed AA, Hassan HM, Belbahri L, Rateb ME, Sayed AM. Flavonoids as potential anti-MRSA agents through modulation of PBP2A: a computational and experimental study. *Antibiotics*. 2020;9(9):1–16. doi:10.3390/antibiotics9090562

25. Humphrey W, Dalke A, Schulten K. Visual molecular dynamics.Pdf. *J Mol Graph*. 1996;14(1):33–38. doi:10.1016/0263-7855(96)00018-5
26. Grant BJ, Rodrigues APC, ElSawy KM, McCammon JA, Caves LSD. Bio3d: an R package for the comparative analysis of protein structures. *Bioinformatics*. 2006;22(21):2695–2696. doi:10.1093/bioinformatics/btl461
27. Mukhtar M, Khan HA, Naz S. Antibacterial profiling of zanthoxylum armatum extracts: a comprehensive computational and experimental study. *Nat Prod Commun*. 2024;19(3):1934578X241237911.
28. Odisitse S, Matshwele JTP, Mazimba O, et al. Nickel mixed ligand complexes against drug resistant bacteria: synthesis, characterization, antibacterial activities and molecular docking studies. *Results Chem*. 2023;6(September):101098. doi:10.1016/j.rechem.2023.101098
29. Zhang S, Qu X, Tang H, et al. Diclofenac resensitizes methicillin-resistant *Staphylococcus aureus* to β-lactams and prevents implant infections. *Adv Sci*. 2021;8(13):1–16.
30. Mahasenan KV, Molina R, Bouley R, et al. Conformational dynamics in penicillin-binding protein 2a of methicillin-resistant *Staphylococcus aureus*, allosteric communication network and enablement of catalysis. *J Am Chem Soc*. 2017;139(5):2102–2110. doi:10.1021/jacs.6b12565
31. Meireles L, Gur M, Bakan A, Bahar I. Pre-existing soft modes of motion uniquely defined by native contact topology facilitate ligand binding to proteins. *Protein Sci*. 2011;20(10):1645–1658. doi:10.1002/pro.711
32. Bornot A, Etchebest C, de Brevern AG. Predicting protein flexibility through the prediction of local structures. *Proteins Struct Funct Bioinforma*. 2011;79(3):839–852. doi:10.1002/prot.22922
33. Fan Q, Yuan Y, Jia H, et al. Antimicrobial and anti-biofilm activity of thymoquinone against Shigella flexneri. *Appl Microbiol Biotechnol*. 2021;105(11):4709–4718. doi:10.1007/s00253-021-11295-x
34. Wang C, Chang T, Yang H, Cui M. Antibacterial mechanism of lactic acid on physiological and morphological properties of *Salmonella enteritidis*, *Escherichia coli* and *Listeria monocytogenes*. *Food Control*. 2015;47:231–236. doi:10.1016/j.foodcont.2014.06.034
35. Zheng X, Guo J, Rao H, et al. Antibacterial and antibiofilm activity of coenzyme Q0 against Vibrio parahaemolyticus. *Food Control*. 2020;109:106955. doi:10.1016/j.foodcont.2019.106955
36. Cheng G, Sa W, Cao C, et al. Quinoxaline 1,4-di-N-oxides: biological activities and mechanisms of actions. *Front Pharmacol*. 2016;7(MAR):1–21. doi:10.3389/fphar.2016.00064
37. Cheng G, Li B, Wang C, et al. Systematic and molecular basis of the antibacterial action of quinoxaline 1,4-di-noxides against Escherichia coli. *PLoS One*. 2015;10(8):1–18.
38. Suter W, Rosselet A, Knuesel F. Mode of action of quindoxin and substituted quinoxaline-di-N-oxides on Escherichia coli. *Antimicrob Agents Chemother*. 1978;13(5):770–783. doi:10.1128/AAC.13.5.770
39. Xu F, Cheng G, Hao H, et al. Mechanisms of antibacterial action of quinoxaline 1,4-di-N-oxides against clostridium perfringens and Brachyspira hyodysenteriae. *Front Microbiol*. 2016;7(DEC):1–12. doi:10.3389/fmicb.2016.01948
40. Dwyer DJ, Belenky PA, Yang JH, et al. Antibiotics induce redox-related physiological alterations as part of their lethality. *Proc Natl Acad Sci*. 2014;111(20):E2100–E2109.
41. Léger L, Budin-Verneuil A, Cacaci M, Benachour A, Hartke A, Verneuil N. β-lactam exposure triggers reactive oxygen species formation in enterococcus faecalis via the respiratory chain component DMK. *Cell Rep*. 2019;29(8):2184–2191. doi:10.1016/j.celrep.2019.10.080